XV International Conference on Durability of Building Materials and Components
DBMC 2020, Barcelona
C. Serrat, J.R. Casas and V. Gibert (Eds)

Ionic Diffusivity and Pore Structure of Hardened Cement Paste Exposed to High Temperature Environment for Long Period

Isao Kurashige

Nuclear Fuel Cycle Backend Research Center, Civil Engineering Research Laboratory,
Central Research Institute of Electric Power Industry, 1646 Abiko, Abiko-shi, Chiba, 270-1194, Japan,
kurasige@criepi.denken.or.jp

Abstract. *Ion diffusion through cement-based barrier is key to safe radionuclide transfer in intermediate radioactive waste disposal facilities. The purpose of this research is to elicit the behavior of ionic diffusivity and pore structure of hardened cement paste specimens for the barrier system when exposed to high temperatures (up to 80°C) for long periods (up to one year). The cement paste is made of an ordinary Portland cement base- and a low-heat Portland cement / fly ash / limestone filler (LF) system. The results of the adsorption isotherms of N_2 and water vapor of the specimens exposed to lime-saturated water of different temperatures, 20, 40, 50, 60, and 80°C, are presented, and their pore size distributions are analyzed by the Barrett-Joyner-Halenda method. The change of specific surface areas is measured and the influence of high temperature on the pore structure is discussed. Additionally, results of chloride ionic diffusivity test for the specimens after the high-temperature exposure are contrasted with the tendency of pore structure change. It is found that the LF system has much higher resistance to high-temperature exposure than ordinary Portland cement; however, temperatures greater than or equal to 60°C deteriorate the ionic diffusivity. These experimental results may indicate the ionic diffusivity of hardened cement paste can be influenced by the spatial electrical charge in micropores depending on the electrical charge of pore wall and the ion composition of pore solution.*

Keywords: *Radioactive Waste Disposal, Cement-Based Barrier, High Temperature, Ionic Diffusivity, Hardened Cement, Microstructure.*

1 Introduction

The microstructure of hardened cement with micro- and nano-sized hierarchical pore structure is not fully understood. The amorphous structure of calcium silicate hydrate (C-S-H), which is the main product of the hydration of cement, is considered one of the reasons for that.

The structure of C-S-H can change due to the hydration and polymerization reactions under the influence of temperature (Scrivener, *et al.*, 2019). Consequently, changes in the microstructure influences the ionic diffusivity in the hardened cement. Evaluation of ionic diffusivity is also a key issue for the design and assessment of a radioactive waste disposal system with a cement-based barrier. Especially, for disposal of heat exothermic radioactive waste, the influence of high temperature on the performance of a cement-based barrier should be thoroughly examined to build a disposal system with high reliability and safety. The temperature of the action depends on the actual concentration of exothermic radionuclides such as cobalt-60 in nuclear waste, assumed to be around 60°C below the design temperature, to prevent excessive influence of temperature on the disposal system. The duration of the exposure to the high temperature can extend over several decades or hundred years. However, until now, few studies have reported on the influence of long-term high temperature on the ionic diffusivity of hardened cement.

Therefore, it is necessary to gain deeper understanding on the behavior of the hardened cement under the high temperature.

The purpose of this study is to investigate the ionic diffusivity of hardened cement exposed to high temperatures over a long period. From the results of the investigation, we discuss the effectiveness of a prime candidate material for the disposal system. The rest of the manuscript is structured as follows: Section 2 discusses the composition of the hardened cementitious specimens and the experimental methodology (adsorption tests and ion-diffusion test). Section 3 produces experimental results and discusses about the pore structure of the specimens exposed to various temperature levels for one year. It also compares the effect of temperature on Cl^- ion diffusivity with that of the pore structure of hardened cement paste.

2 Materials and Methods

2.1 Materials

The cement-based barrier for the nuclear waste disposal system should be durable and denser, experience little shrinkage, and have low hydration heat among others, for enhancing the barrier performance. In this context, two specimens of cement paste were prepared with a water-binder mass ratio (W/B) of 0.45, as shown in Table 1. The first specimen was made of ordinary Portland cement. The second specimen was made of low-heat Portland cement, which is a mix of siliceous fly ash and lime stone filler (fly ash binder mass ratio (FA/B) = 0.30: lime stone filler powder mass ratio (LS/P) = 0.38). LF30 is a prime candidate mix for the nuclear waste disposal system.

The specimens were cast in molds of $2 \times 2 \times 8$ cm^3 volume. They were then demolded and subsequently stored in a saturated atmosphere at 20°C for one year, for an adequately mature hydration reaction. This is because the high temperature condition in a nuclear disposal facility occurs after the backfill closure of the disposal tunnel. After curing, the specimens were immersed in lime-saturated water at 20, 40, 50, 60, and 80°C for one year.

Table 1. Mix proportions of cement paste.

Mix code	W/B	W/P	FA/B	LS/P
OPC	0.45	0.45	-	-
LF30		0.28	0.30	0.38

2.2 Methods

2.2.1. Nitrogen gas and water vapor adsorption tests

For the adsorption test, the specimens were ground into particles of size 106-500 μm and degassed at 105°C in vacuum for 24 h. Adsorption tests with N_2 gas and water vapor were carried out using Quantachrome instruments autosorb iQ and VSTAR, respectively. The measurement temperatures were 77 K for N_2 adsorption and 293 K for H_2O vapor adsorption.

The pore size distribution (2 nm to 500 μm) was determined by the Barrett-Joyner-Halenda (BJH) method using the N_2 desorption isotherm data. In addition, from adsorption isotherms of N_2 and H_2O, based on the Brunauer-Emmett-Teller theory, under a relative pressure (P/P_0) of 0.05-0.30, the specific surface areas of the specimens were calculated.

2.2.2. Measurement of effective diffusion coefficient of Cl^- ions

The effective diffusion coefficient of Cl^- ions of the specimens after exposure was measured by the steady-state penetration-type diffusion test, with a concentration difference of 1,700 ppm of Cl in lime-saturated NaCl solution at 20˚C. Samples for the diffusion test were cut to 2 × 2 × 0.5 cm^3 and saturated in lime water under vacuum for one day. The effective diffusion coefficient was determined when the diffusion was in steady sate. The test time to reach equilibrium was less than six months for OPC and more than one year for LF30.

3 Results and Discussion

3.1 Adsorption Isotherms and Microstructure of Cement Paste

3.1.1. Nitrogen adsorption isotherms

The measured N_2 adsorption isotherms of the OPC and LF30 specimens are shown in Figures 1 and 2, respectively. According to the classification of adsorption isotherms by IUPAC, these isotherms correspond to type IV(a), the type of hysteresis loop in their isotherms have characteristics of both H2(a) and H2(b) as pore blocking/percolation effects and evaporation via cavitation in a relative pressure range of 0.42 to 0.50 are indicated (Cychosz, *et al.*, 2017).

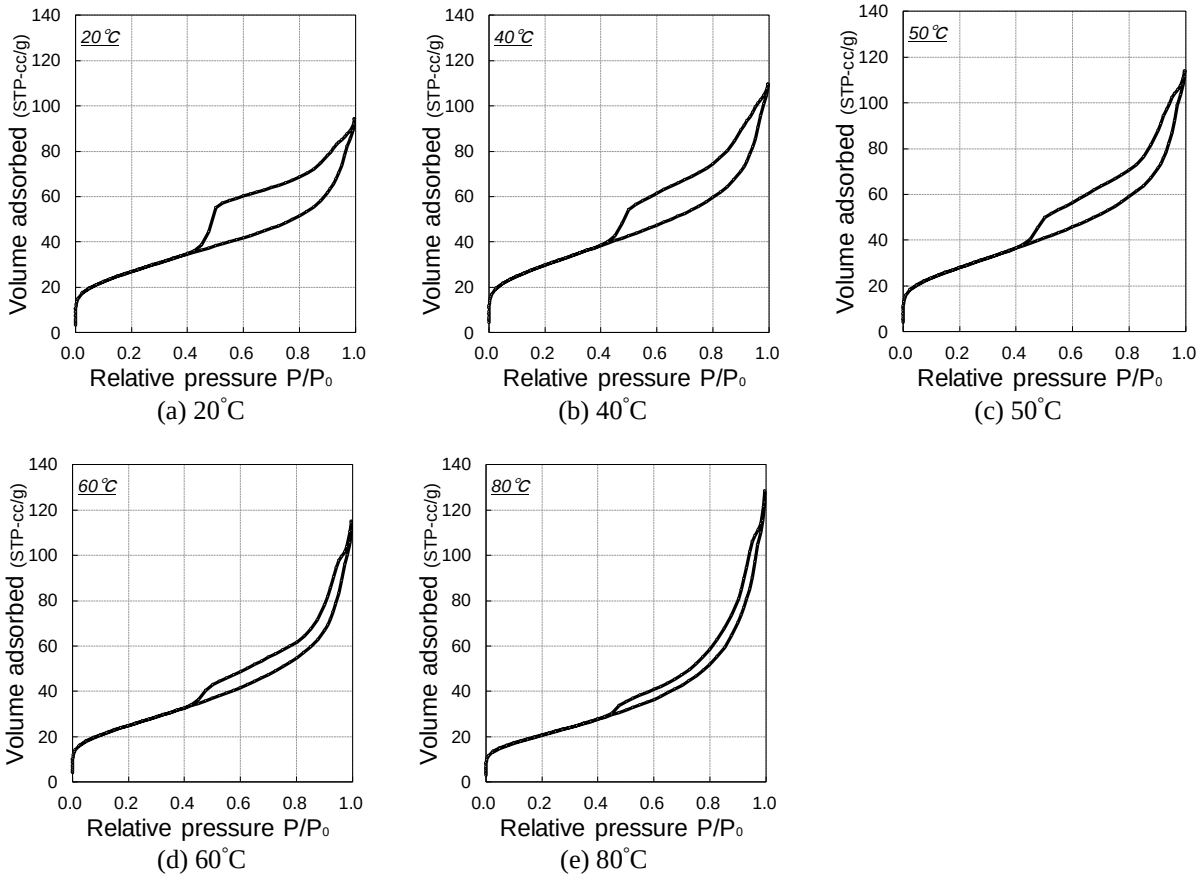

Figure 1. N_2 gas adsorption isotherms of OPC specimens exposed to various temperature conditions.

On the one hand, as shown in Figure 1, it is evident that the level of exposure temperature has a significant impact on the N_2 adsorption isotherms of OPC where higher temperature makes the hysteresis weak and remarkably reduces the desorption volume via cavitation. These changes are presumably due to the coarsening of the pore structure with expanded neck pores as well as a simplified pore network with ink-bottle-shaped pores (Gallucci, *et al.*, 2013). On the other hand, the isotherms of LF30 in Figure 2 are not influenced by the temperature so much as OPC, indicating the superiority of mix proportion of LF30 on resistance to high temperatures. Since solid-state ^{29}Si NMR detected the reaction progress of unreacted fly ash in LF30 during the high temperature exposure, the change for the worse in pore structure of LF30 could be reduced by the healing effect of fly ash.

Figure 3 illustrates pore size distributions determined for the different specimens and temperatures by the BJH method. A clear difference in the pore size distributions of OPC due to the exposure to high temperature can be seen Figure 3 (a), where higher temperature leads to an increase of gel pores around 10 to 50 nm. It should be noted that the sharp peaks at approximately 4 nm do not correspond to the actual pore in the specimens, which is an apparent peak calculated from the drastic evaporation via cavitation. The total pore volumes as well as the change in pore size distribution in LF30 are smaller than those in OPC.

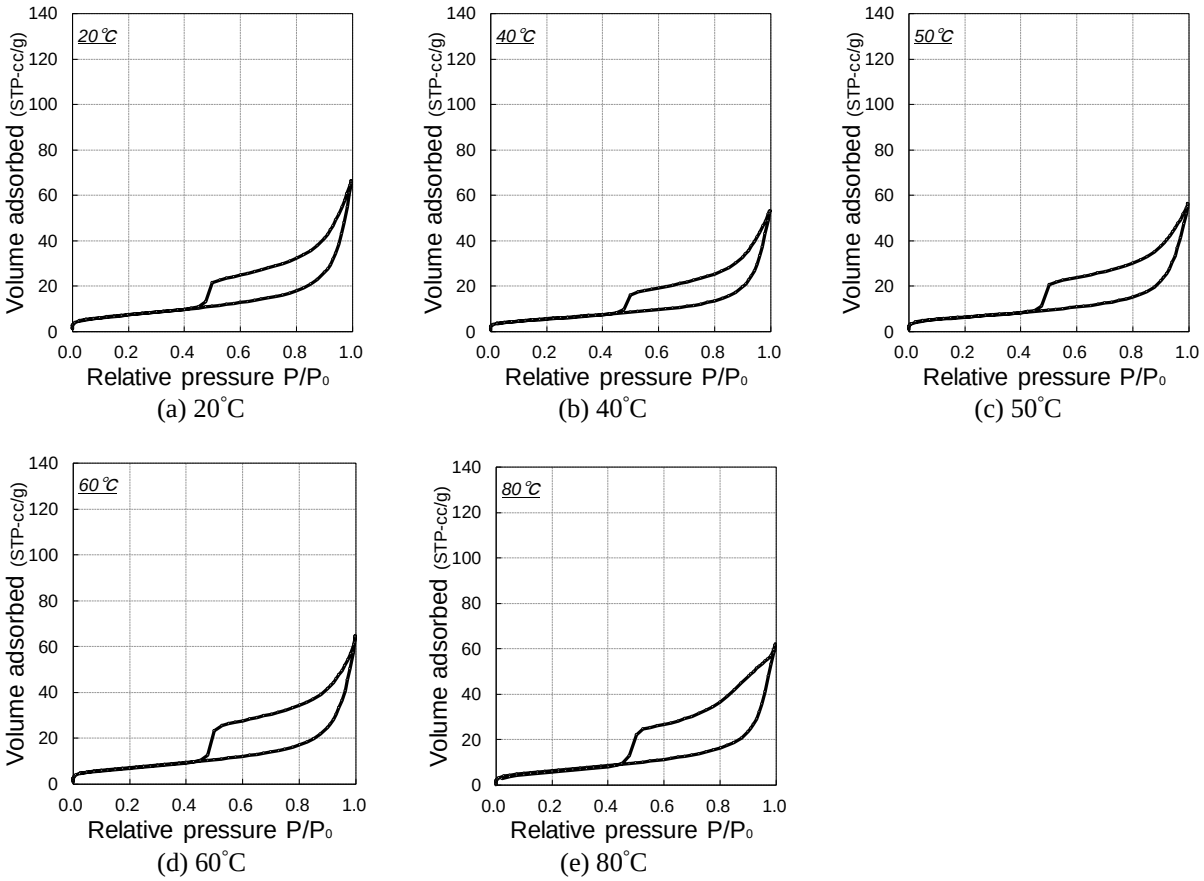

Figure 2. N_2 gas adsorption isotherms of LF30 specimens exposed to various temperature conditions.

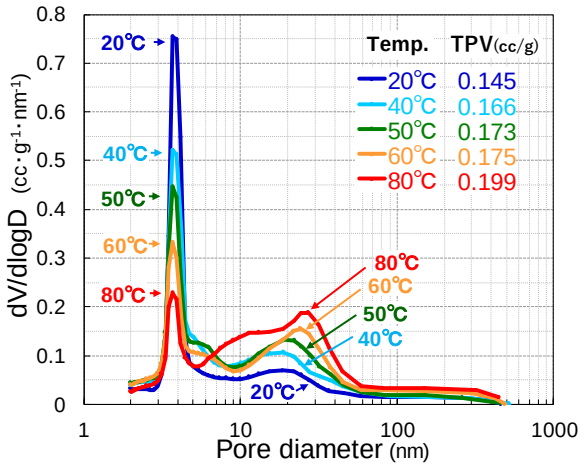

(a) OPC

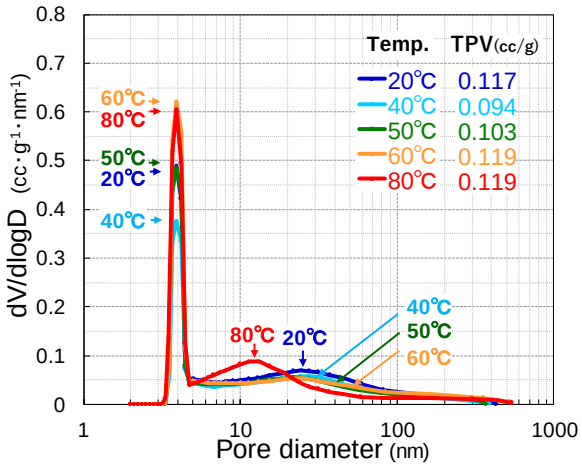

(b) LF30

Figure 3. Pore size distributions calculated from N_2 gas desorption isotherms.

3.1.2. Water vapor adsorption isotherms

Adsorption isotherms of water vapor in Figure 4 show a similar trend with those of the N_2 gas. In the case of OPC, volume of drastic desorption shown at P/P_0 = approximately 0.35 is found to be smaller at the higher temperature, which can be due to the cavitation of water (Maruyama, *et al.*, 2018). The difference in the isotherms of LF30 is found to be smaller than those of OPC. This trend is similar to that of the N_2 gas adsorption isotherms. The adsorption volume remained uniform at P/P_0 = 0.05 in the desorption branch of OPC is decreased with higher temperature level. This result indicates that the water retention capacity of the OPC specimens can be degraded by high temperature. By contrast, in the case of LF30, this trend is not clear except at 80°C.

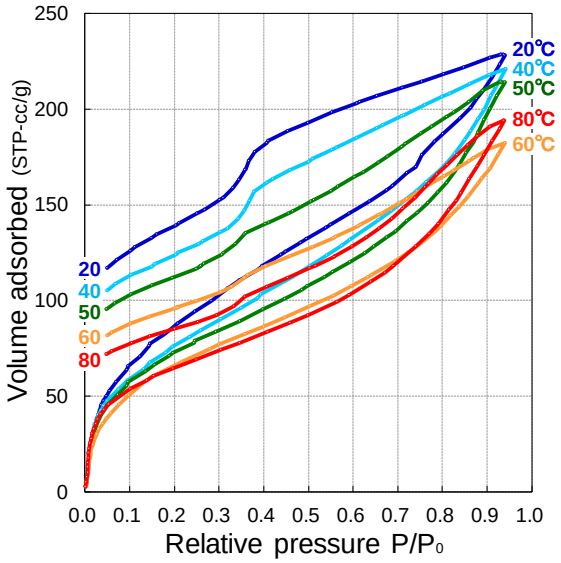

(a) OPC

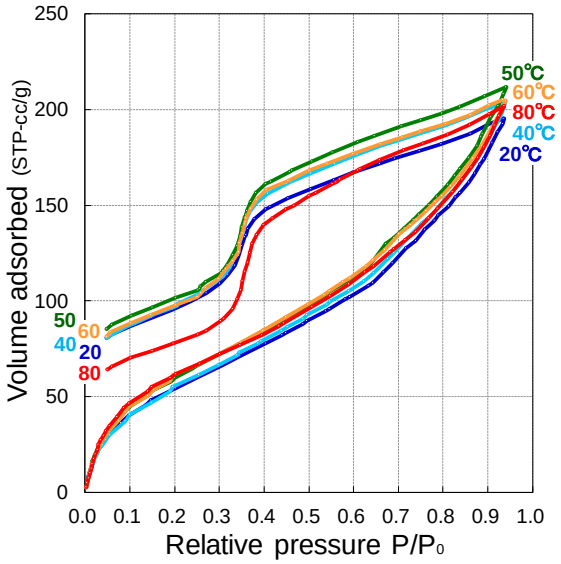

(b) LF30

Figure 4. Water vapor adsorption isotherms of specimens exposed to various temperature conditions.

3.1.3. Specific surface area

BET surface areas of N_2 and H_2O for all specimens can be compared in Figure 5. Water molecules smaller than N_2 molecules can access narrower pores than the accessible size (approximately 0.45 nm diameter calculated from the cross-section area of N_2 molecule). Therefore, from Figure 5, BET surface areas of H_2O for any specimens is larger than that of N_2. The decrease in the BET areas of N_2 and H_2O for OPC when exposed to high temperature was caused by polymerization of the silicate chains in C-S-H (Gallucci, *et al.*, 2013), which was

detected by the NMR measurement. In contrast, in the case of LF30, there were no significant changes in the BET surface areas. However, as with OPC, the NMR detected the polymerization of C-A-S-H under higer temperature.

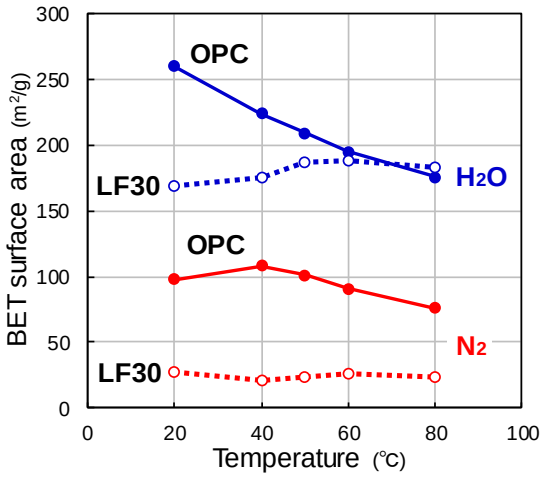

Figure 5. BET surface areas obtained from N_2 gas and water vapor adsorption isotherms.

3.2 Chloride Ionic Diffusivity

The effective diffusion coefficient of Cl^- ions, D_{cl} in the specimens are shown in Figure 6. The results revealed that D_{cl} of LF30 is nearly four orders of magnitude lower than that of OPC, when exposed to temperatures below 50°C. On the other hand, the influence of temperature varied with the specimen; higher the temperature, larger the D_{cl} of OPC. On the other hand, D_{cl} of LF30 slightly increased at 60°C and significantly at 80°C. This increase of does not agree with the trend of change in pore structure shown in subsection 3.1. Hence, a clear understanding about the mechanism of this phenomenon is needed. It is recognized that the incorporation of aluminum in fly ash modifies the structure of C-S-H (C-A-S-H) and also the surface charge (L'Hopital, *et al.*, 2015). Moreover, the surface charge and ionic composition in pore solution have a strong influence on the ionic diffusion through hardened cement, especially when the microstructure is very dense (Yang, *et al.*, 2019). Furthermore, the decomosition of AFt and AFm phases and its influence on the ionic compositon in pore solution and ionic diffusivity should be discussed for this mix proportion and materials.

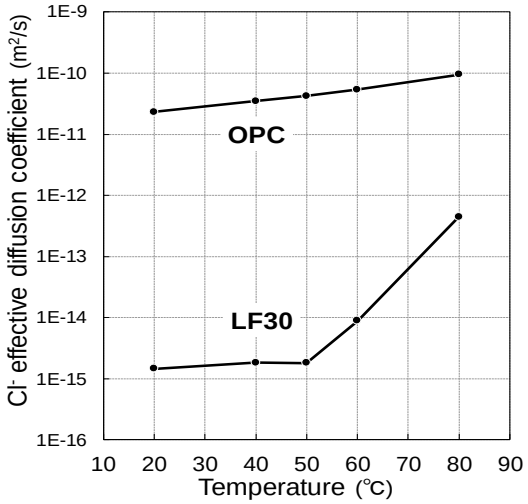

Figure 6. Effective diffusion coefficients of Cl^- ions.

4 Conclusions

- In the case of OPC, the pore size distribution determined from N_2 gas desorption isotherms using the BJH method shows obvious temperature-dependent coarsening of the microstructure of hardened cement. In the case of LF30, temperature had a negligible influence on the microstructure, except at 80°C.
- BET surface area of OPC calculated from N_2 gas and water vapor adsorption isotherms decreased with temperature. In contrast, the BET surface area of LF30 had low sensitivity to temperature.
- The Cl^- ionic diffusion coefficient of OPC increased with temperature. The coefficient of LF30 is nearly four orders of magnitude lower than that of OPC below 50°C. However, the value slightly increased at 60°C and significantly at 80°C.

ORCID

Isao Kurashige: http://orcid.org/0000-0002-2773-0885

References

Cychosz, K.A., Guillet-Nicolas, R., Garcia-Martinez, J. and Thommes, M. (2017). Recent advances in the textural characterization of hierarchically structured nanoporous materials. *Royal Society of Chemistry*, 46, 389-414.

Gallucci, E., Zhang, S. and Scriviner, K. (2013). Effect of temperature on the microstructure of calcium silicate hydrate (C-S-H), *Cement and Concrete Research*, 53, 185-195.

L'Hopital, E., Lothenbach, E., Le Saout, G., Kulik, D. and Scrivener, K. (2015). Incorporation of aluminium in calcium-silicate-hydrates, *Cement and Concrete Research*, 75, 91-103.

Maruyama, I., Rymes, J., Vandamme, M. and Coasne, B. (2018). Cavitation of water in hardened cement paste under short-term desorption measurements, *Materials and Structures*, 51, 159.

Scrivener, K., Ouzia, A., Juilland, P. and Mohamed, A.K. (2019). Advances in understanding cement hydration mechanisms, *Cement and Concrete Research*, 124, 105823.

Ynag, Y., Patel, R.A., Churakov, S.V., Prasianakis, N.I., Kosakowski, G. and Wang, M. (2019). Multiscale modeling of ion diffusion in cement paste: electrical double layer effects, *Cement and Concrete Composites*, 96, 55-65.